www.czasopisma.pan.pl PAN POLSKA AKADEMIA NAUK www.journals.pan.pl

PAN ARCHIVES OF ACOUSTICS
Vol. **45**, No. 4, pp. 733–746 (2020)
DOI: 10.24425/aoa.2020.135279

Technical Note

Analysis on Acoustic Disturbance Signals Expected During Partial Discharge Measurements in Power Transformers

Michał KUNICKI

Opole University of Technology
Institute of Electrical Power Engineering and Renewable Energy
Opole, Poland
*Corresponding Author e-mail: m.kunicki@po.opole.pl

(*received July 26, 2019; accepted June 1, 2020*)

This paper presents comparative analysis of various acoustic signals expected during partial discharge (PD) measurements in operating power transformer. Main purpose of the paper is to yield relevant and reliable method to distinguish between various acoustic emission (AE) signals emitted by PD and other sources, with particular consideration of real-life results rather than laboratory simulations. Therefore, selected examples of real-life AE signals registered in seven different power transformers, under normal operation conditions, within few years are showed and analyzed. Five scenarios are investigated, which represent five types of AE sources: PD generated by artificial sources, and next four real-life sources (including PD in working transformer, oil flow, oil pumps and core). Several different signal processing methods are applied and compared in order to identify the PD signals. As a result, an energy patterns analysis based on the wavelet decomposition is found as the most reliable tool for identification of PD signals. The presented results may significantly support the process of interpretation of the PD measurement results, and may be used by field engineers as well as other researchers involved in PD analysis using AE method. Finally, observed properties also provide a solid basis for establishing or improving complete classification method based on the artificial intelligence algorithms.

Keywords: acoustic emission; partial discharge; insulation system; measurements; power transformers.

1. Introduction

Partial discharge (PD) is commonly known as one of the most destructive phenomenon affecting high voltage insulation systems (Kunicki *et al.*, 2018; Murugan, Ramasamy, 2015; Tenbohlen *et al.*, 2016). Since adequately early PD detection in the highest priority electric power equipment (e.g. power transformers) may reduce the probability of the system failure, thus it is a crucial issue regarding reliable electric power delivery. Various different methods for PD detection and analysis are presently applied not only in case of laboratory research but also for on-site measurements (Kozioł *et al.*, 2019; Kunicki, Nagi, 2017; Kunicki, 2019; Mondal, Kumbhar, 2018; Rozga, 2016; Yaacob *et al.*, 2014). Acoustic emission method (AE) has become one of the most commonly used methods for few decades, and known as one of the most non-invasive methods that may be applied during normal operating conditions, without having to turn off the diagnosed device – contrary to other methods, which require temporary overhaul of the tested unit (Boczar *et al.*, 2014; Cichoń *et al.*, 2014; Glowacz *et al.*, 2018; Olszewska, Witos, 2012, 2011). Furthermore, it is still the only method that is fully applicable for PD localization under on-site conditions (Coenen, Tenbohlen, 2012; Kraetge *et al.*, 2013; Kunicki *et al.*, 2018; Mehdizadeh *et al.*, 2013). Despite the above-mentioned advantages, AE method also has some limitations, for example: no charge calibration has been possible so far (however, research in this field has been ongoing for several years (Witos, Gacek, 2005)), relatively low sensitivity which indirectly results in quite high relative sensibility to external disturbances (compering to e.g. UHF method) (Calcara *et al.*, 2017; Kunicki *et al.*, 2018; Tenbohlen *et al.*, 2016). Also, not all of the PD defects may be detected by the AE method – usually, it is quite difficult to receive acoustic signals generated by internal PD that occur around the internal parts of

the windings, using commonly applied joint sensors, due to high attenuation of the acoustic wave inside of the transformer – only approx. 1% of the AE signal energy that reaches the transformer tank is transferred to sensor, while 99% is reflected due to the impedance mismatch between oil and steel (Institute of Electrical and Electronics Engineers [IEEE], 2019). Application of the oil-immersed sensors is one of the partial solutions to this issue (e.g. hydrophones), but possibilities for placing them inside the transformer tank are still not optimal in terms of the potential performance of the method (Siegel *et al.*, 2017; Sikorski, 2019).

On-site PD detection in transformers is usually accompanied by many external and internal disturbances that may occur within the device being diagnosed. In order to ensure relevant interpretation of registered signals it is essential to distinguish PD generated signals from others. Several contemporary research works deal with de-noising of the AE signals. Many different algorithms are proposed, usually based on artificial neural networks, fuzzy logic or wavelet decomposition (Búa-Núñez *et al.*, 2014; Ibrahim *et al.*, 2012; Kraetge *et al.*, 2013; Kunicki, Cichon, 2018; Mondal, Kumbhar, 2018). Which is also typical, usually PD signals are generated under laboratory conditions, so their source is known in advance. Identification (or classification) of the PD source is another issue that is readily analyzed in current studies (Harbaji *et al.*, 2015; Kundu *et al.*, 2012; Kunicki *et al.*, 2016; Rubio-Serrano *et al.*, 2012). Also, it is usually limited to several scenarios based on selected artificial PD sources analyzed in laboratory conditions. Despite the fact that analysis of acoustic signals generated by PD in on-site working conditions is quite rarely published, one may point some relevant studies in that matter (Coenen, Tenbohlen, 2012; Kunicki *et al.*, 2018; Nicoară *et al.*, 2016). From a practical point of view, a certain deficiency may be observed in relation to investigations of other AE signals which may occur during acoustic PD measurements in a working power transformer – minor papers deal with that issue (Borucki, 2012; Cichoń *et al.*, 2014; Mahmood Najafi *et al.*, 2013; Olszewska, Witos, 2016). Even the latest IEEE guide on the acoustic PD measurements does not discuss any of the disturbances potentially expected during on-site measurements (IEEE, 2019). So, it seems essential to be sure that captured signal is actually emitted by PD and not by another source – as a result, the objective of this paper is to propose how to effectively and reliably distinguish between AE signals emitted by PD and other sources.

Therefore, in this paper several examples of selected real-life AE signals registered in power transformers during normal exploitation routine tests are presented. Various examples of acoustic signals associated with various sources expected during PD measurements in an operating power transformer are discussed. Furthermore, they were compared with signals emitted by artificial as well as real PD sources.

2. Instruments and methods

2.1. Measuring instruments

All of the results presented and discussed in this paper were registered using typical measuring system, which is widely used for PD measurements on-site and in the laboratory. The setup consists of AE piezoelectric joint sensor mounted on the outer wall of the transformer tank, connected to the amplifier, via a preamplifier, and then to the acquisition unit (Fig. 1).

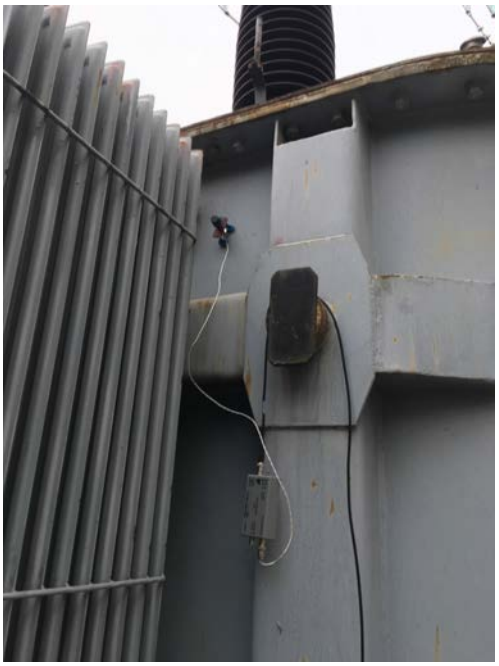

Fig. 1. General view of the measuring instruments during on-site power transformer measurements.

Due to the fact that all the results analyzed in Sec. 3 were recorded over several years on different test objects, the sensors used differ in some scenarios: usually D9241A sensor was used, but also R15α and WD (all made by PAC). Moreover, one of the scenarios uses a high-sensitivity Omicron AES 75 sensor with an integrated preamplifier – in this case no additional preamplifier was used, and sensor was directly connected to the amplifier. All other instruments were the same during all of the tests: preamplifier 2/4/6, amplifier AE2A (both made by PAC) and PicoScope 5443B digital measuring interface. Regarding the interface configuration, its sampling frequency was set to 1 MHz, and measuring window was set to 20 ms – both were constant in all of the tests, which is also crucial issue in terms of further post-processing and analysis (especially using discrete wavelet transform (DWT)).

2.2. Methods of the analysis

The original source signals that were analyzed in all scenarios were the time series of AE signals generated by various sources. Then, typical signal processing, commonly used for PD signal analysis, was applied (Boczar *et al.*, 2014; Harbaji *et al.*, 2013; 2015; Kunicki, 2019; Witos *et al.*, 2011): amplitude spectrum based on the fast Fourier transform (FFT), spectrograms based on the short time Fourier transform (STFT) and energy pattern analysis based on the DWT. Because typical analysis based only on FFT, STFT and time runs did not give clear possibilities to distinguish signals generated by different sources, a simple classification method based on the energy patterns using DWT was applied. Similar method was presented in (Kundu *et al.*, 2013; Li *et al.*, 2013; Shang *et al.*, 2017; Veloso *et al.*, 2008), but authors proposed identification of different PD types, without taking into account any of the disturbances that may occur during on-site tests. Regarding the DWT analysis, Symlets wavelet family was used, because it is widely recognized as one of the optimal solutions for PD signal analysis – sometimes Daubechies wavelets are also proposed as an equivalent tool (Boczar *et al.*, 2014; Kundu *et al.*, 2012; Li *et al.*, 2013). After several surveys wavelet filter order was set to 16, and it was an optimal solution – further increasing the filter order did not yield any significant improvement in minimizing the aliasing. AE generated by PD usually occurs in the frequency band between approx. 30 kHz and 150 kHz, however some researchers gave examples of PD signals which also show the share of higher frequency components, in the 300–400 kHz range (Boczar *et al.*, 2014; Kunicki *et al.*, 2018; Witos *et al.*, 2011). According to the contemporary knowledge and experience of the author, upper frequency of the DWT analysis was set to 500 kHz – considering the Nyquist theorem and applied sampling frequency of 1 MHz. Six levels of decomposition were carried out – Table 1 presents approximated frequency bands of each detail.

Table 1. Approximated frequency bands of each detail coefficients of the DWT.

Detail coefficients	Approximated frequency band [kHz]
cD1	500–250
cD2	125–250
cD3	63–125
cD4	31–63
cD5	16–31
cD6	0–16

Next, energy patterns were determined based on the DWT – the energy share of each detail in the total signal energy was determined. Final results are assigned for 3000 sample signals in each scenario (including various voltage levels, in case of laboratory tests presented in Subsec. 3.1). Next step was to fit the probability distribution of the analyzed data. The generalized extreme value distribution (GEV) delivered the best fit. GEV is commonly used to estimate the smallest or largest value among a large set of independent, identically distributed random values representing measurements or observations. It is quite universal tool that combines three simpler distributions into one form, giving a continuous range of possible shapes, which include all three of the simpler distributions: exponential distributions – e.g. normal distribution; polynomial distributions – e.g. Student's t distribution; finite distributions – e.g. the beta distribution. Having the optimal distribution model, it was possible to assign confidence intervals to the expected values of each detail – according to the stochastic nature of the PD, 90% confidence interval was proposed and marked in the plots in Sec. 3.

3. Results and discussion

In the presented study five scenarios were analyzed: PD generated by artificial source in laboratory conditions, PD generated by real-life PD source in working power transformer, AE generated by oil flow in working power transformer, AE generated by oil pumps in working power transformer, and AE emitted by core.

3.1. Signals generated by artificial PD source

This section compares the three commonly studied artificial PD sources: needle-needle (NN), needle-plate (NP) – grounded plate electrode, and surface discharge generated on the pressboard paper (SRF) – rod-plate system with pressboard plate between electrodes. All PDs were generated in new mineral transformer oil. Figure 2 presents exemplary time runs of the AE signals emitted by three selected artificial sources. Analyzed window was set to 20 ms, which corresponds to one period of 50 Hz supply voltage – therefore, it is typical value in most European power systems. Presented patterns are typical AE wave forms emitted by PD – two main activity zones may be noticed, related to rising slope of each halfcycle of supply voltage. Due to the lack of synchronization of the AE signals with voltage phase during the measurements, it is not possible to distinguish which polarity of the supply voltage is associated with the first and second 10 ms of the analyzed signals. Generally, AE signals emitted by the selected artificial PDs are quite similar to each other, when analyzed in time domain – no explicit differences may be noticed.

Frequency domain analysis brings some more relevant information related to each of the applied PD sources (Fig. 3). According to NN and NP, frequency

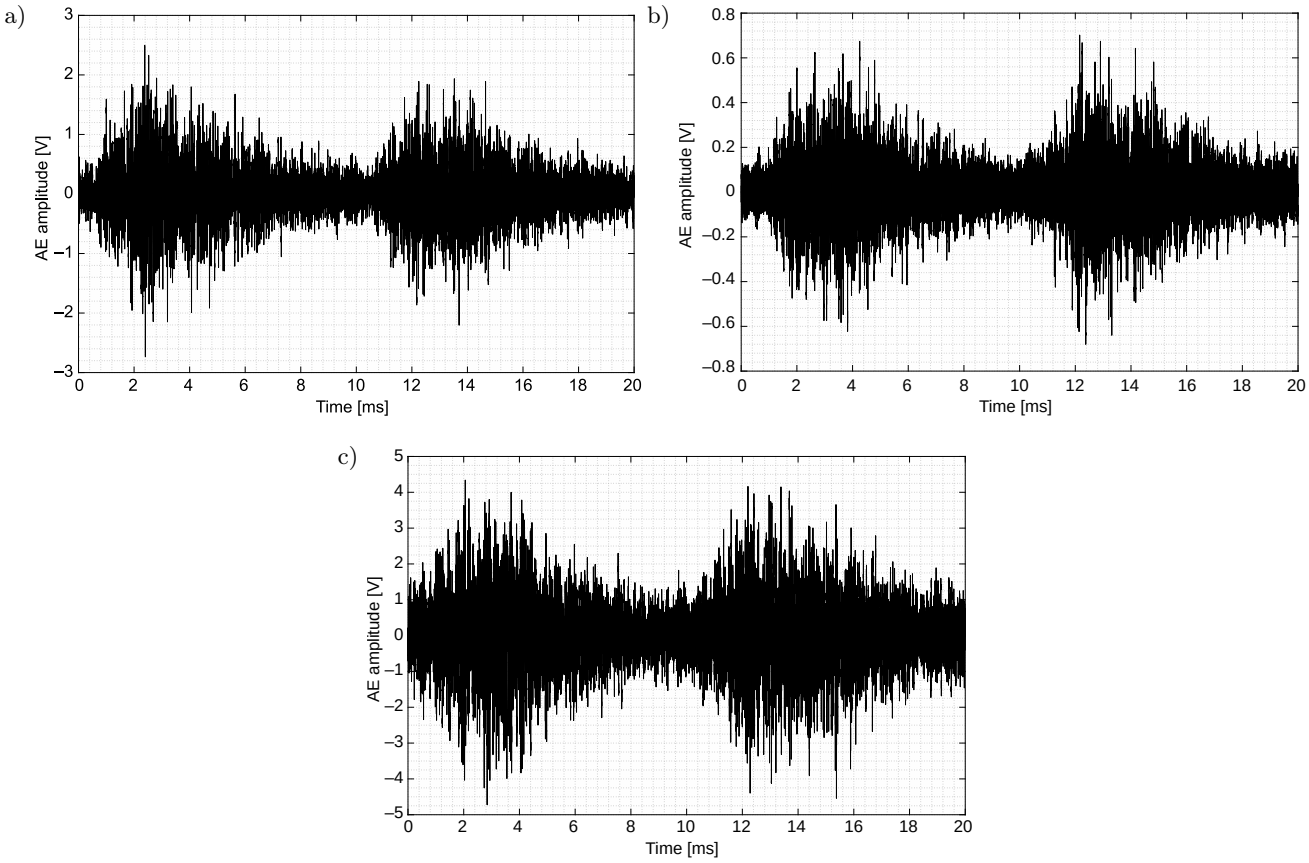

Fig. 2. Representative time runs of the AE signals generated by selected PD sources: a) NN, b) NP, c) SRF.

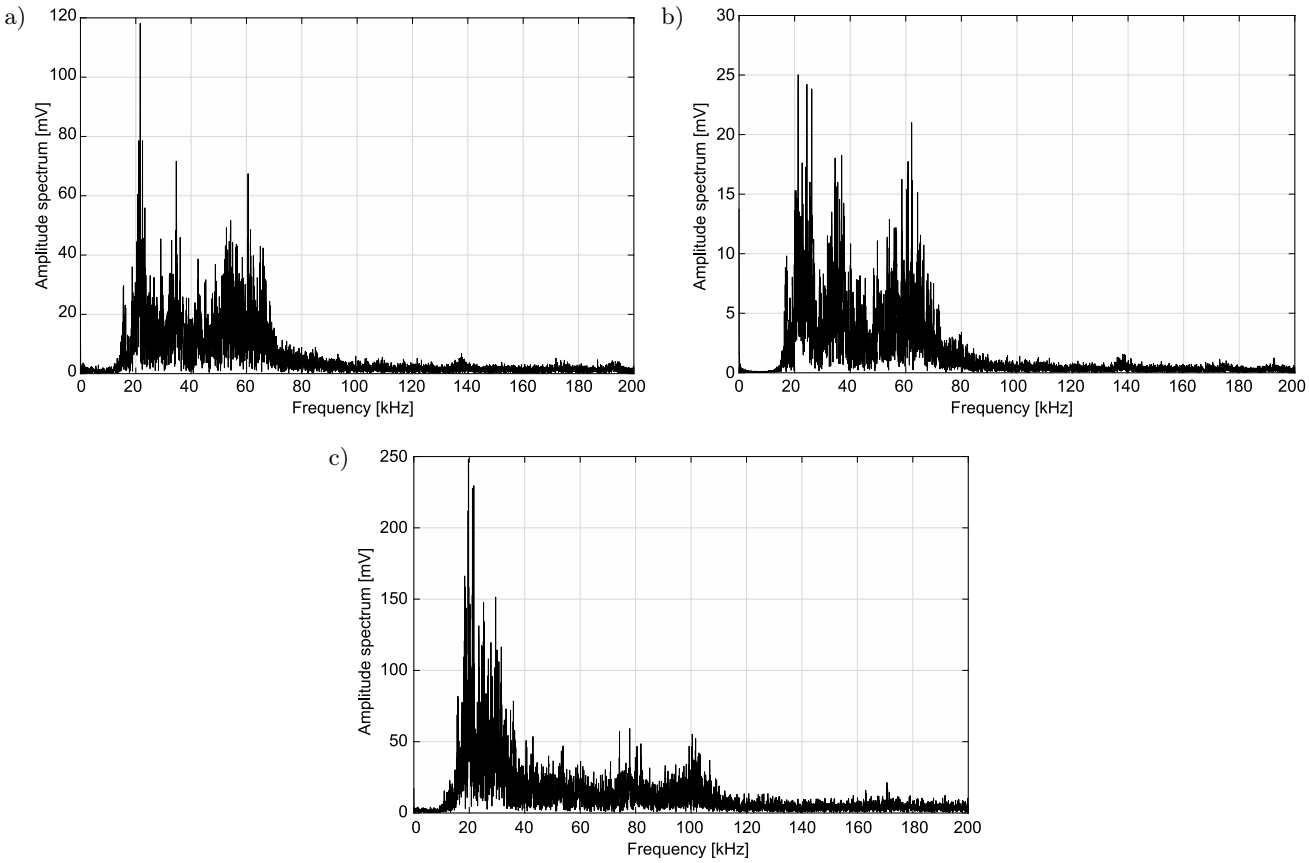

Fig. 3. Representative amplitude spectrums of the AE signals generated by selected PD sources: a) NN, b) NP, c) SRF.

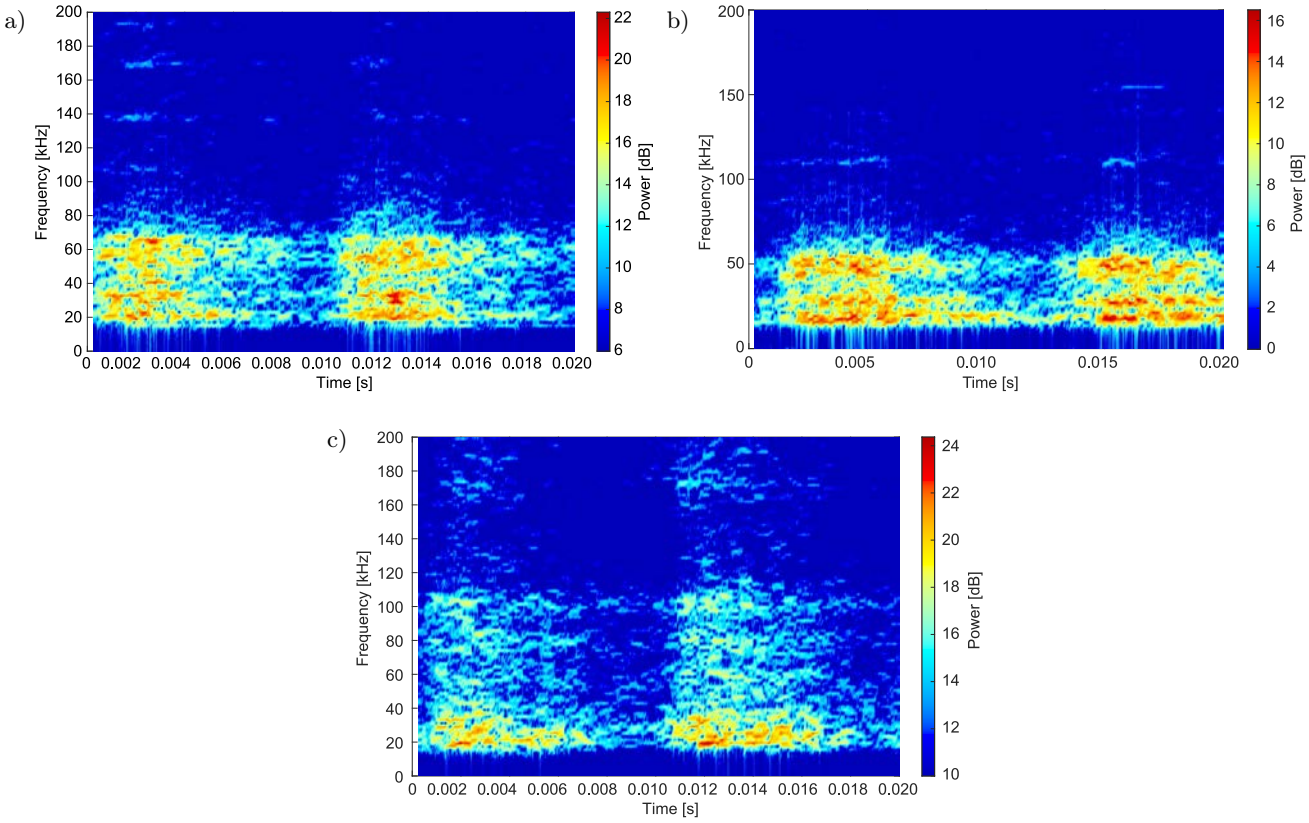

Fig. 4. Representative spectrograms of the AE signals generated by selected PD sources: a) NN, b) NP, c) SRF.

range of the highest activity is similar, and is about 20–70 kHz, with three evident local peaks (approx. 25 kHz, 35 kHz and 55 kHz). In case of SRF scenario, the band is significantly wider and covers 20–110 kHz, with domination of the 20–40 kHz contents, while 40–110 kHz tail is significantly damped comparing to the dominant band – this tail is related to the surface phenomenon that occurs on the abutment of three environments: galvanic electrode, liquid dielectric and solid dielectric. A dominant band is related to the part of the energy that is associated with PD in oil.

STFT was used as the next typical signal analysis tool. It did not bring any significant observations – generally, it confirmed most of the remarks revealed during spectrum analysis. Furthermore, as it could be expected, duration of the selected frequency content of the signal decreases with the frequency raise – low frequency contents last much longer than high frequency contents (which complies with the theory of the AE propagation in liquids), but in case of NN differences in duration are the lowest.

The most explicit description of the investigated signals was yielded by the energy patterns analysis based on DWT (Fig. 5). Three dominant details may be observed as the most relevant in all scenarios: cD3, cD4 and cD5. Moreover, proportions between shares of those details in their sum (or total sum of the signal energy) may be used to distinguish between those sources. These results are in accordance with results presented by other researchers, where AE signals emitted by artificial PDs under laboratory conditions were analyzed (Kundu *et al.*, 2012; Veloso *et al.*, 2008).

3.2. Signals generated by real-life PD

As analysis of the AE signals generated by artificial PD has been quite widely presented in many publications so far, it is essential to compare whether these results and conclusions may be applied to real-life signals emitted by PD in power transformer. Figure 6 presents exemplary time runs of the AE signals generated by PDs in working power transformers (unit 1 – 115/16.5 kV 25 MVA, and unit 2 – 115/16.5 kV 16 MVA). In both scenarios presence of PDs has been confirmed by advanced diagnostic methods (i.e. electrical method, UHF method, dissolved gas method and internal inspection), so the presented results are reliable.

Signals appear at 10 ms intervals, which confirms the discussion carried out in Subsec. 3.1. It is also characteristic that signals are much more damped than those registered in laboratory (tail is shorter), which was affected by higher environmental attenuation of the source signal in the transformer tank – it is especially visible in the case of internal PD in paper (Fig. 6b), which usually is very difficult to detect by

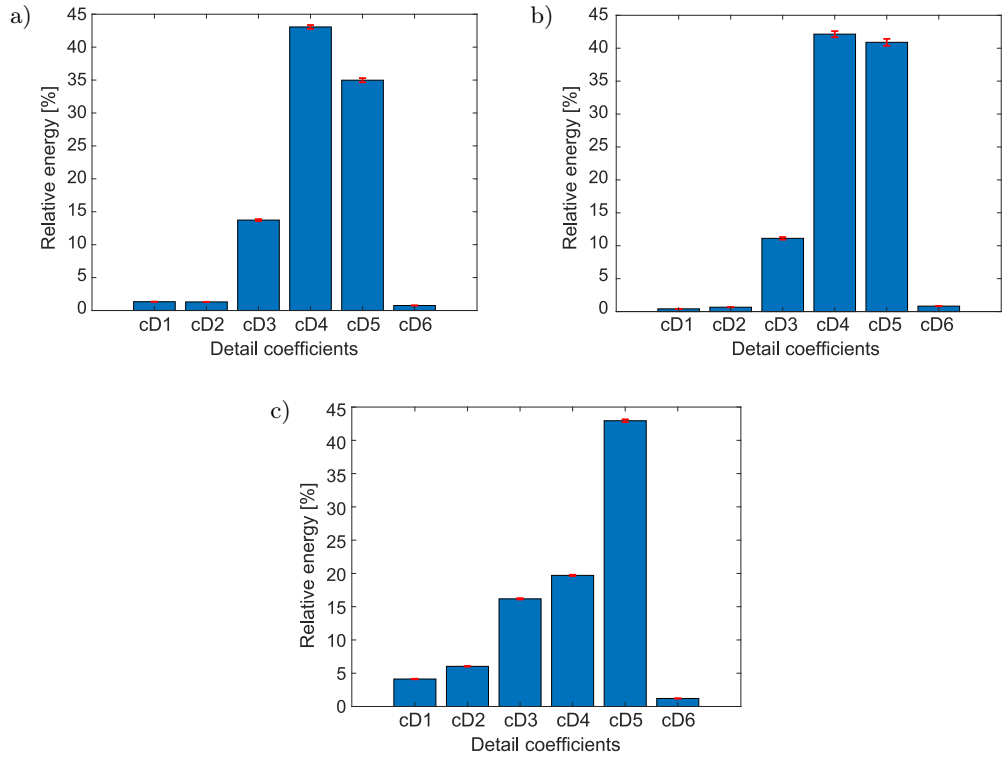

Fig. 5. DWT based energy patterns of the AE signals generated by selected PD sources: a) NN, b) NP, c) SRF.

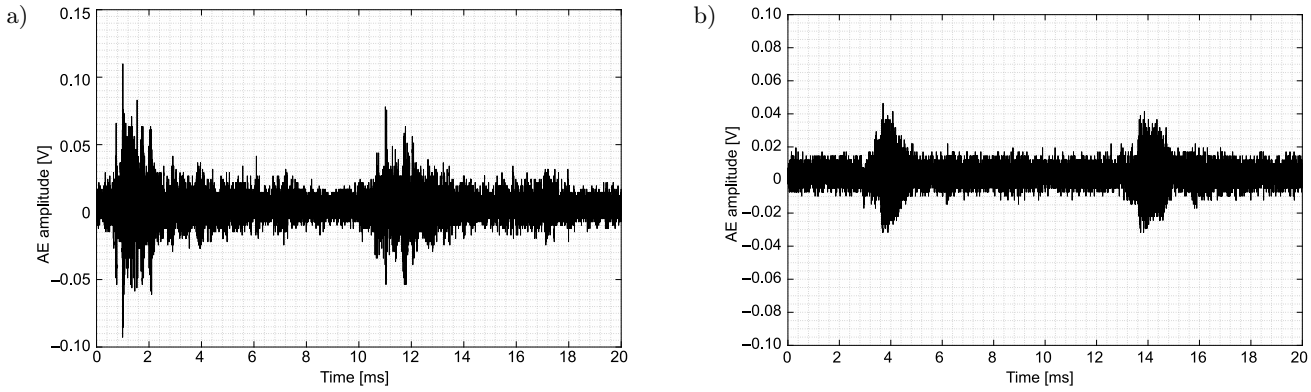

Fig. 6. Representative time runs of the AE signals generated by real-life PD sources in power transformer: a) surface discharge in oil (unit 1), b) discharge in paper (unit 2).

AE method due to strong attenuation. Also, results presented in Figs 7 and 8 are quite interesting. They show frequency and time-frequency domain analysis respectively. Defect related to unit 1 is characterized by the highest activity band around 20–80 kHz, which also appeared in case of laboratory results discussed in Subsec. 3.1. Contrary situation may be observed in case of the second defect related to unit 2 – very narrow band signal was captured, around 45 kHz, and other contents are hardly noticeable. The most probable reason was that the path between source and sensor (various different environments and barriers) created a resonant band-pass filter that made the source signal not only attenuated but also filtered. Such situation could be possible when AE was emitted by internal PD occurred in paper insulation (around the windings).

Regarding the DWT analysis (Fig. 9), in the case of surface discharges, one can observe relatively good convergence of results, when comparing it to an artificial PD source (Fig. 9a) – the same three details are dominant: approx. share of cD3 is 18% in both lab and on-site scenarios, also cD4 shares are similar (22% and 24% in lab and on-site scenario, respectively), while cD5 shares significantly differ. Due to the significant loss of original source information, resulting from the propagation path, no significant conclusion may be drawn about the results shown in Fig. 9b – results should not be generalized or extended to other objects.

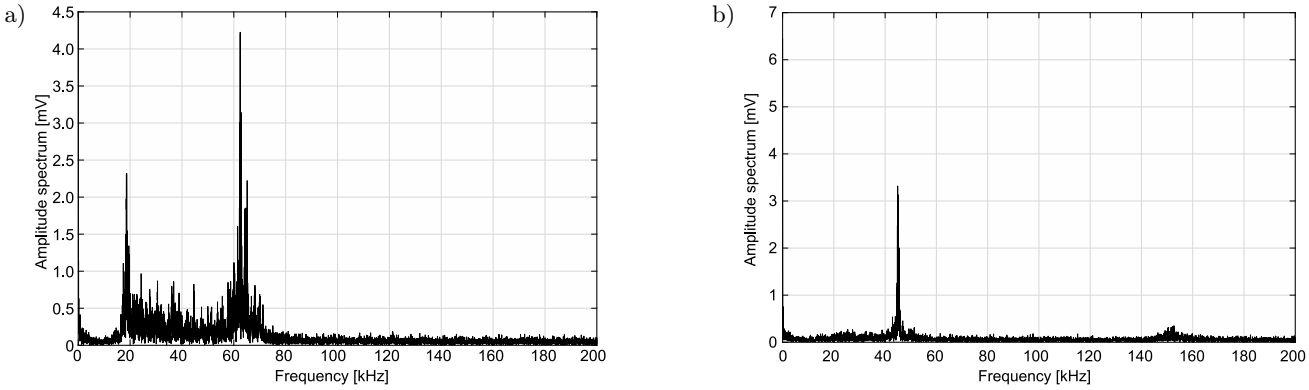

Fig. 7. Representative amplitude spectrums of the AE signals generated by real-life PD sources in power transformer: a) surface discharge in oil (unit 1), b) discharge in paper (unit 2).

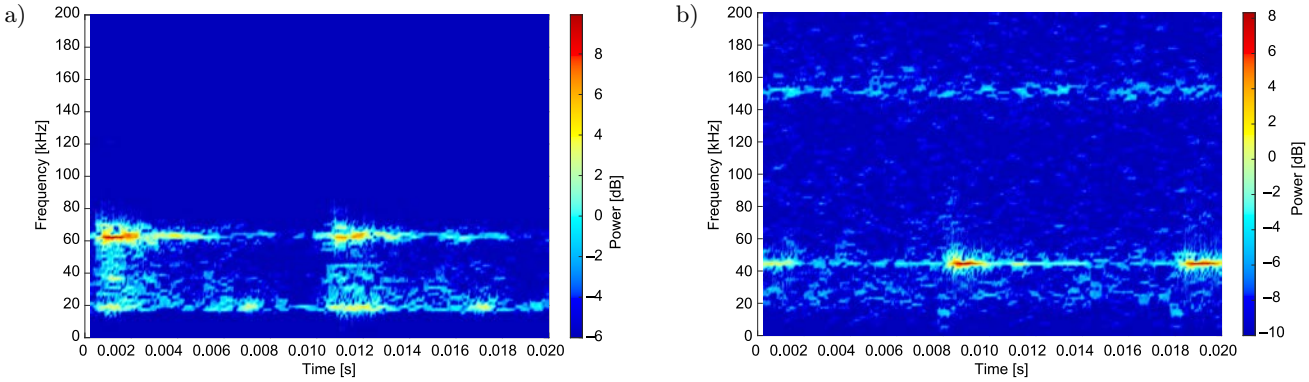

Fig. 8. Representative spectrograms of the AE signals generated by real-life PD sources in power transformer: a) surface discharge in oil (unit 1), b) discharge in paper (unit 2).

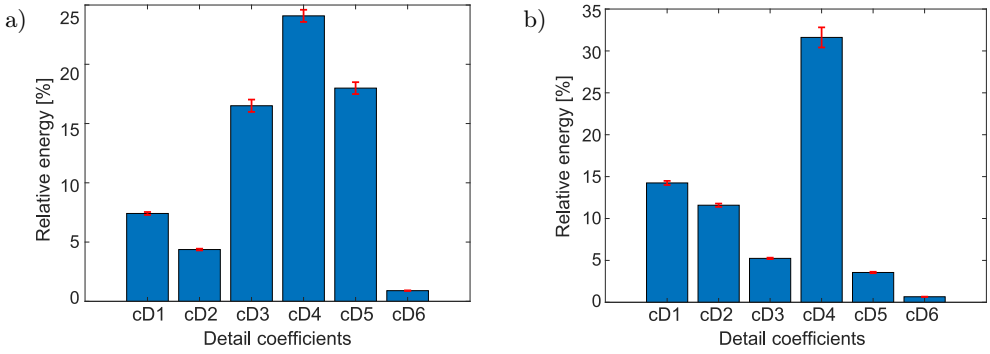

Fig. 9. DWT based energy patterns of the AE signals generated by real-life PD sources in power transformer: a) surface discharge in oil (unit 1), b) discharge in paper (unit 2).

3.3. Signal generated by oil flow

The first type of these disturbance signals that can potentially be expected when measuring PD in a power transformer is AE generated by the oil flow. Such signals usually occur when environment volume of the circulating oil rapidly changes (usually rapidly increases or decreases) – e.g. pipe from radiators enters the tank: then high oil turbulences may appear, and depending on the oil flow density, they may emits AE. As mentioned above, these kind of signals are usually expected near cooling system joints with the main tank, or when some of the valves or locks do not work properly (e.g. they are not fully open or otherwise interfere with normal oil flow). Two different examples of the AE signals generated by oil flow in two different working power transformers (unit 3 – 115/15.7/6.3 kV, 25/16/16 MVA, unit 4 – 125/13.8 kV, 150 MVA) are presented in Fig. 10.

At glance, time runs of the signals registered in unit 3 (Fig. 10a) are quite similar to PD signals – activity presented in 10 ms intervals. Significantly differ-

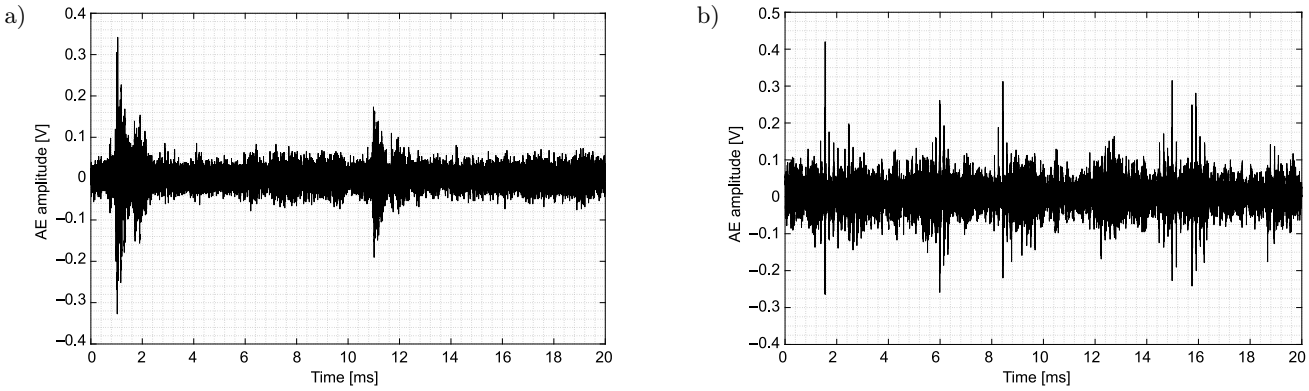

Fig. 10. Representative time runs of the AE signals generated by oil flow in power transformer: a) unit 3, b) unit 4.

ent wave forms may be observed regarding the unit 4 (Fig. 10b) – there are repetitive signals at each approx. 7 ms mixed with much weaker pulses at each 3 ms. Spectrum analysis (Fig. 11) and STFT (Fig. 12) also confirm that nature of both analyzed signals is different, despite they are emitted by similar sources: unit 3 shows narrow band emission focused around 23 kHz, while unit 4 brings evident harmonic type behavior with the same 23 kHz basic frequency and additionally its next 4 harmonics.

Finally, to confirm if there are any similarities between the two signals, DWT based energy patterns were analyzed (Fig. 13). Contrary to the time and frequency analysis, energy patterns yielded relatively similar results. Four details coefficients are essential for further analysis: cD5, cD4, cD3 (the same as in case of PDs) and cD1. One may note that ratio of cD5 to cD4 is approx. 1:3, as well as ratio cD4 to cD4 is around 1:2 in both units, having regard to the confidence boundary of the details coefficients. Another interesting observation is that AE signals generated by oil flow are much more random than those emitted by PD. Comparing confidence boundaries in oil flow scenario it is evident that they are significantly

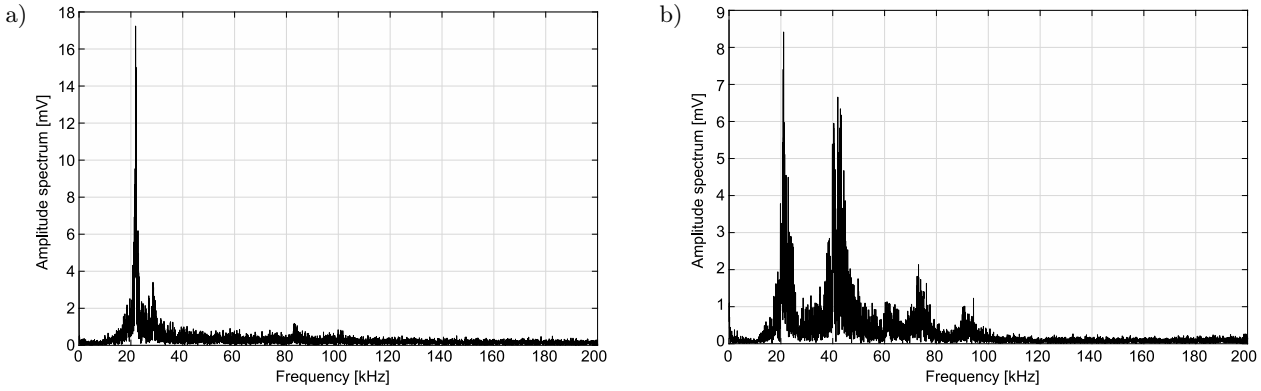

Fig. 11. Representative amplitude spectrums of the AE signals generated by oil flow in power transformer: a) unit 3, b) unit 4.

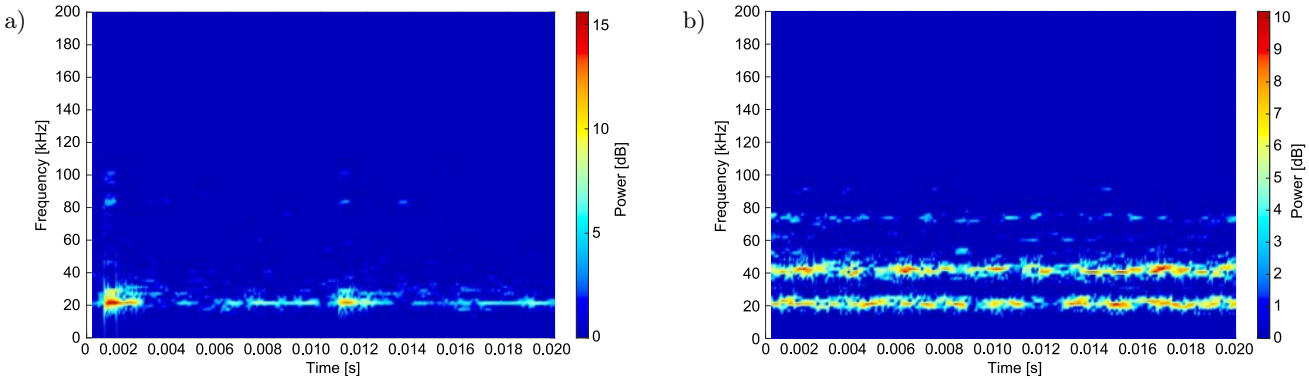

Fig. 12. Representative spectrograms of the AE signals generated by oil flow in power transformer: a) unit 3, b) unit 4.

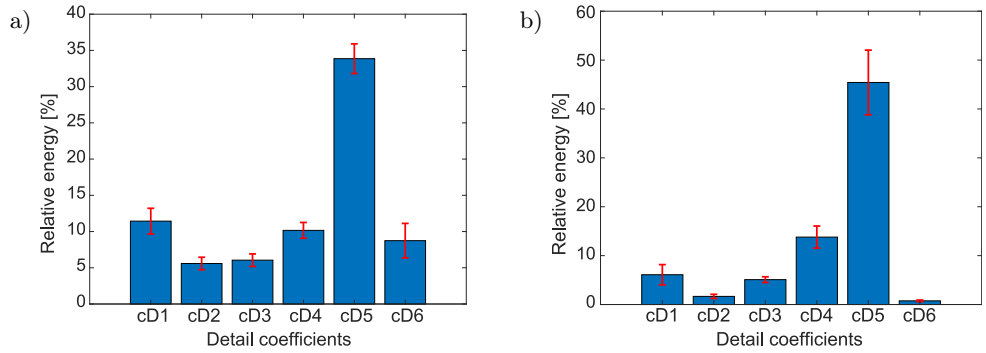

Fig. 13. DWT based energy patterns of the AE signals generated by oil flow in power transformer: a) unit 3, b) unit 4.

more spread out than in PD scenarios. It is because AE signals tightly depend on the temporary oils flow conditions (temperature, flow density, pressure, etc.) which vary in dynamic way, and are generally less determined than PD generation condition in the particular moment.

3.4. Signals generated by oil pumps

Next scenario shows exemplary AE signals generated by oil pump in unit 5: 125/13.8 kV and 150 MVA transformer (Fig. 14). According to the high-to-medium voltage transformers, oil pumps may be usually met in larger units (usually 40 MVA and above), where oil-forced air-forced (OFAF) cooling system is used more often, contrary to oil-natural air-forced (ONAF) commonly used in smaller units.

In the analyzed scenario, pumps were powered directly by 50 Hz power grid, with no variable frequency drive (VFD), so it was expected that the emitted AE signals would be synchronized with the supply voltage phase. As a result, one may observe highest AE activity in 10 ms, regular intervals (Fig. 14a), similar to PD wave forms. It should be emphasized that expected interval in this kind of signals depends on the pump power supply frequency (not the grid frequency), thus

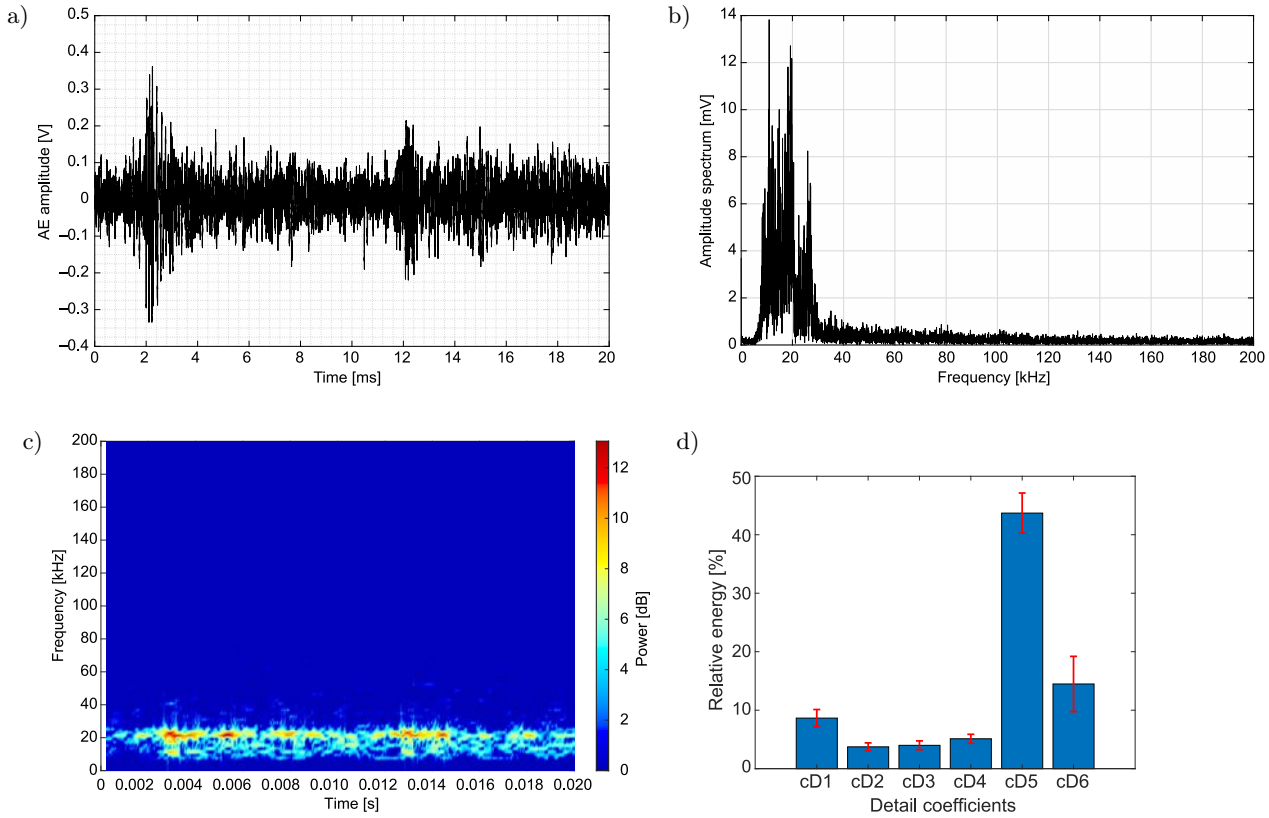

Fig. 14. Analysis of the signals emitted by oil pump in unit 5: a) time run, b) amplitude spectrum, c) spectrogram, d) DWT based energy patterns.

if VFD is used, other, much shorter or longer intervals may be expected, when higher or lower frequencies are applied respectively. This kind of signals are also characterized by the dominance of low frequency content (in fact, acoustic band rather than ultrasonic), which is confirmed by Figs 14b and 14c. Also DWT analysis yielded similar information: most of the energy is related to details cD5 and cD6 – where source signal is presented. Detail coefficients associated with higher frequencies relate to noise rather than the source signal.

3.5. Signals generated by core

Last of the analyzed scenarios deals with two types of signals generated by transformer magnetic core: AE by magnetostriction in unit 6 (125/6.3 kV, 40 MVA), and AE by loose element in core of the unit 7 (121/16.5/6.3 kV, 40/27/40 MVA). Exemplary time runs of the AE signals emitted by two defects related to core are presented in Fig. 15. One may notice two different wave forms with different repetitive intervals: 4 ms in case of unit 6 (Fig. 15a) and 10 ms in case of unit 7 (Fig. 15b). AE registered in unit 6 are typical signals generated as a result of the magnetostriction phenomenon – results are in good agreement with those presented in (Olszewska, Witos, 2016), where similar signals are analyzed, and also further physical theory of the phenomenon is provided. According to the results achieved for unit 7, a loose element around bottom of the iron sheets of the core has been diagnosed and confirmed by additional vibration testing. In case of unit 6, the most dominant frequency band is approx. 15–40 kHz, while in case of unit 7 it is narrower: 15–30 kHz (Figs 16 and 17).

Again, the most interesting observations are related to the energy patterns analysis (Fig. 18). It turned out that thanks to DWT analysis it was revealed that the relative energy share of the coefficient details is almost identical in both cases. It is quite interesting especially according to that fact that both signals were related to different phenomenon. It may be explained that energy contents of the AE signals in this cases (and probably others also) depend on the source properties (material, environment, geometry, etc.) rather than on the physical phenomenon that excites the source – despite that time runs and mean frequency spectrums were significantly different, an adequate energy patterns analysis showed that both signals come from similar source (iron sheets of the core).

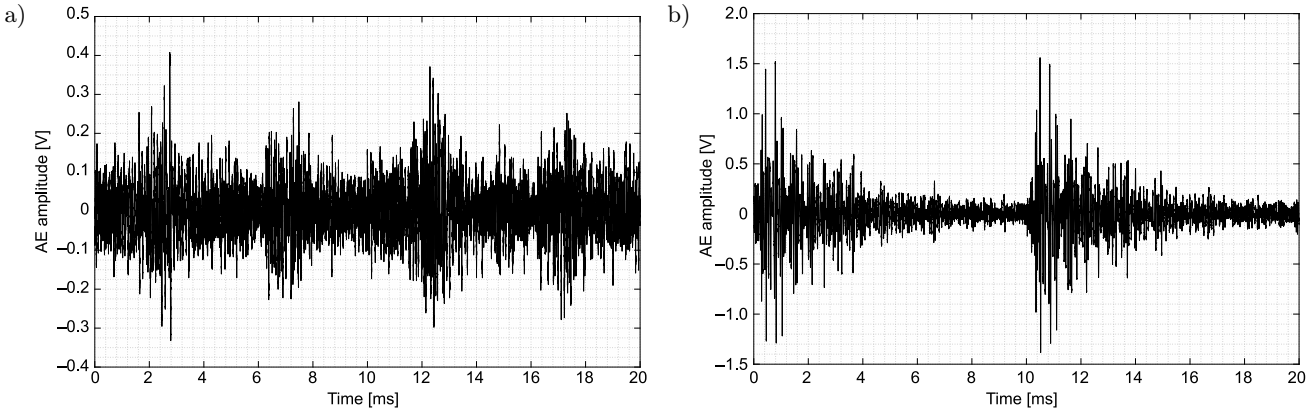

Fig. 15. Representative time runs of the AE signals generated by core in power transformer: a) magnetostriction (unit 6), b) loose element (unit 7).

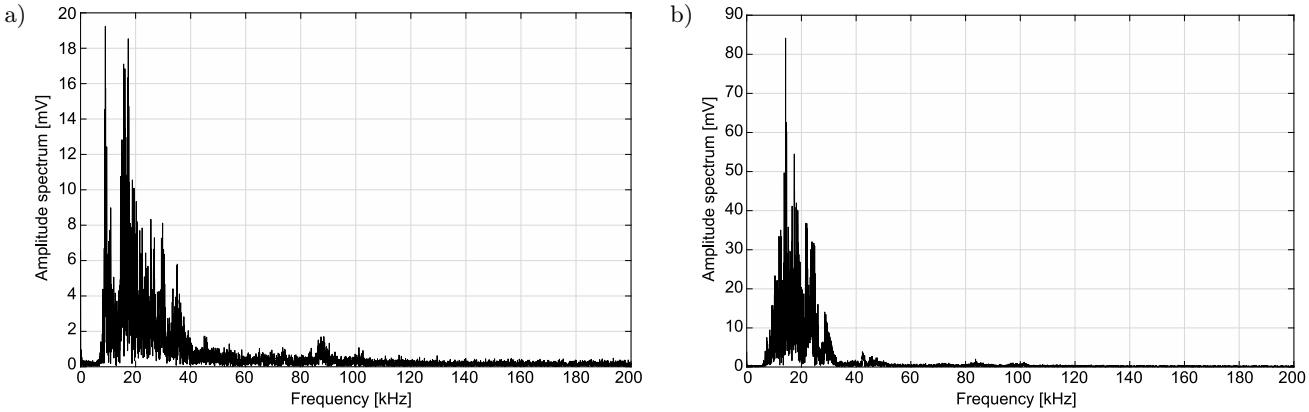

Fig. 16. Representative amplitude spectrums of the AE signals generated by core in power transformer: a) magnetostriction (unit 6), b) loose element (unit 7).

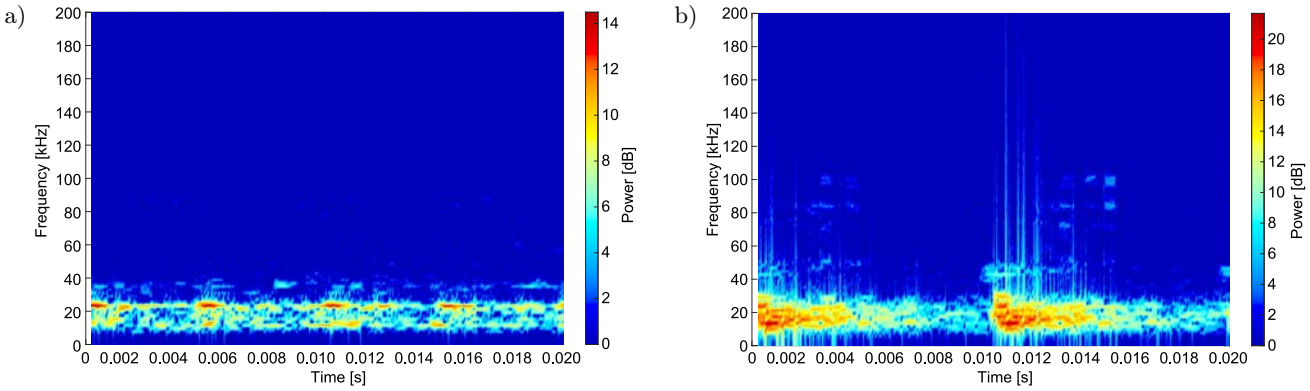

Fig. 17. Representative spectrograms of the AE signals generated by core in power transformer: a) magnetostriction (unit 6), b) loose element (unit 7).

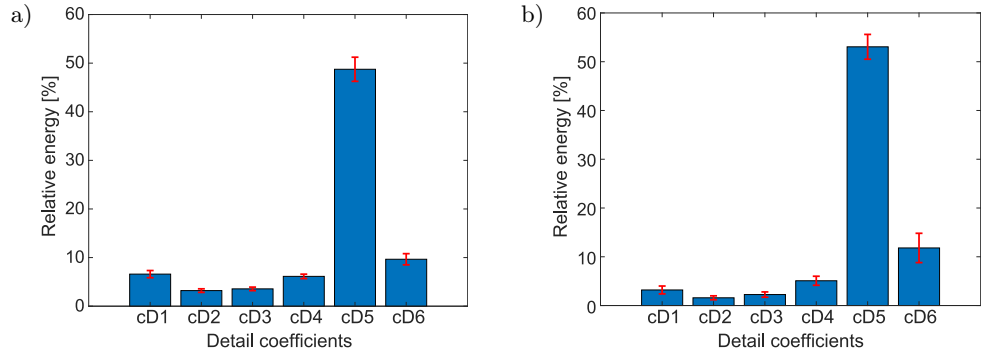

Fig. 18. DWT based energy patterns of the AE signals generated by core in power transformer: a) magnetostriction (unit 6), b) loose element (unit 7).

3.6. Possible applications of the presented results

This section summarizes and gather all the results presented above, and shows the potential of these results in proposing a classification method. Table 2 presents confidence boundaries of the detail coefficients in relation to all of the defects that were represented in previous sections. The coefficients are normalized, and expressed in values between 0 and 1.

Figure 19 illustrates conception of the exemplary classification method, which uses three selected and normalized coefficient details. This simple method is based on the clustering, and is used just to demonstrate potential further applications of the presented results.

Table 2. Normalized confidence boundaries of the detail coefficients in relation to the selected defects.

Defects	Normalized 90% confidence boundaries of the relative energy for the detail coefficients					
	cD1	cD2	cD3	cD4	cD5	cD6
NN	0.0132 0.0135	0.0129 0.0132	0.135 0.139	0.427 0.434	0.346 0.353	0.0074 0.0078
NP	0.0041 0.0042	0.0065 0.0068	0.109 0.114	0.416 0.426	0.403 0.415	0.0080 0.0086
SRF	0.040 0.042	0.059 0.061	0.160 0.163	0.196 0.198	0.427 0.432	0.011 0.013
PD	0.140 0.145	0.113 0.118	0.051 0.053	0.300 0.329	0.345 0.365	0.0064 0.0068
Oil flow	0.040 0.132	0.012 0.065	0.045 0.069	0.090 0.161	0.318 0.520	0.010 0.110
Pumps	0.071 0.101	0.030 0.044	0.032 0.048	0.043 0.059	0.402 0.472	0.097 0.192
Core T3	0.023 0.074	0.018 0.036	0.017 0.039	0.041 0.066	0.462 0.556	0.085 0.148

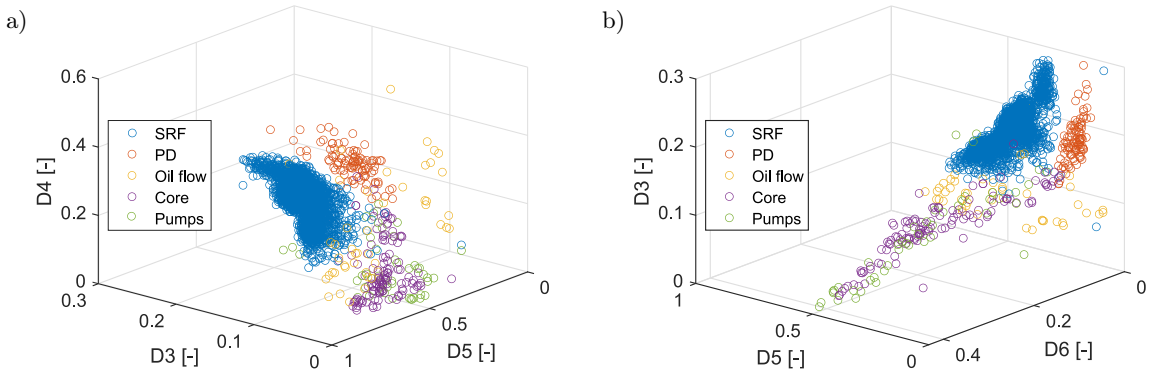

Fig. 19. Exemplary classification method based on 3D clustering of the energy patterns using selected details: a) cD3, cD4, cD6, b) cD3, cD5, cD6.

As one may notice it is possible to select some unique regions associated with each type of signals, in which the probability of occurrence is the highest – data from Table 2 may be used as initial values in optimization process of the clustering regions.

4. Conclusion

1) This article compares and analyzes several examples of acoustic signals recorded in operating power transformers that may significantly affect and disturb the PD measurements. Five different scenarios were discussed, including artificial PD, real-life PD, AE emitted by oil flow, pumps and core. As a result, the essential information was obtained about key differences between the signals generated by PD and others that can be recorded during on-site testing. The key contribution of this paper may be identified as follows:
   - AE emitted by artificial PDs can be used as a reference database only at the initial stage of testing (e.g. classification), due to the possibility of some significant differences in relation to real signals – this should be verified by means of an appropriate database containing actual confirmed real-life signals.
   - According to proposed measurement methodology (DWT analysis) the most important (in terms of identification of the signal source) are detail coefficients cD5, cD4 and cD3.
   - Energy patterns analysis based on the DWT yielded the most explicit information about the investigated signals, thus it may be used for classification purposes.
   - Conventional time and frequency domain analysis is not precise enough to distinguish between PD signals and other presented in this contribution.
   - Energy contents of the AE signals generated by core depend on the source properties rather than on the physical phenomenon that excites the source.
2) Finally, presented results may significantly support identification of the source signals during the acoustic testing of the power transformers in normal exploitation conditions.

Acknowledgment

The work was co-financed from funds of the National Centre for Research and Development in Poland (NCBR) as part of the Tango 4 project (TANGO-IV-A/0005/2019-00).

References

1. Boczar T., Cichon A., Borucki S. (2014), Diagnostic expert system of transformer insulation systems using the acoustic emission method, *IEEE Transactions on Dielectrics and Electrical Insulation*, **21**(2): 854–865, doi: 10.1109/TDEI.2013.004126.
2. Borucki S. (2012), Diagnosis of technical condition of power transformers based on the analysis of vibroacoustic signals measured in transient operating conditions, *IEEE Transactions on Power Delivery*, **27**(2): 670–676, doi: 10.1109/TPWRD.2012.2185955.
3. Búa-Núñez I., Posada-Román J.E., Rubio-Serrano J., Garcia-Souto J.A. (2014), Instrumentation system for location of partial discharges using acoustic detection with piezoelectric transducers and optical fiber sensors, *IEEE Transactions on Instrumentation and Measurement*, **63**(5): 1002–1013, doi: 10.1109/TIM.2013.2286891.
4. Calcara L., Pompili M., Muzi F. (2017), Standard evolution of Partial Discharge detection in dielectric liquids, *IEEE Transactions on Dielectrics and Electrical Insulation*, **24**(1): 2–6, doi: 10.1109/TDEI.2016.006499.

5. Cichoń A., Borucki S., Wotzka D. (2014), Modeling of acoustic emission signals generated in on load tap changer, *Acta Physica Polonica A*, **125**(6): 1396–1399, doi: 10.12693/APhysPolA.125.1396.
6. Coenen S., Tenbohlen S. (2012), Location of PD sources in power transformers by UHF and acoustic measurements, *IEEE Transactions on Dielectrics and Electrical Insulation*, **19**(6): 1934–1940, doi: 10.1109/TDEI.2012.6396950.
7. Glowacz A., Glowacz W., Glowacz Z., Kozik J. (2018), Early fault diagnosis of bearing and stator faults of the single-phase induction motor using acoustic signals, *Measurement: Journal of the International Measurement Confederation*, **113**: 1–9, doi: 10.1016/j.measurement.2017.08.036.
8. Harbaji M., El-Hag A., Shaban K. (2013), Accurate partial discharge classification from acoustic emission signals, *2013 3rd International Conference on Electric Power and Energy Conversion Systems, EPECS 2013*, pp. 4–7, doi: 10.1109/EPECS.2013.6713000.
9. Harbaji M., Shaban K., El-Hag A. (2015), Classification of common partial discharge types in oil-paper insulation system using acoustic signals, *IEEE Transactions on Dielectrics and Electrical Insulation*, **22**(3): 1674–1683, doi: 10.1109/TDEI.2015.7116364.
10. Ibrahim K., Sharkawy R.M., Salama M.M.A., Bartnikas R. (2012), Realization of partial discharge signals in transformer oils utilizing advanced computational techniques, *IEEE Transactions on Dielectrics and Electrical Insulation*, **19**(6): 1971–1981, doi: 10.1109/TDEI.2012.6396955.
11. Institute of Electrical and Electronics Engineers (2019), *IEEE Guide for the detection, location and interpretation of sources of acoustic emissions from electrical discharges in power transformers and power reactors*, IEEE Std C57.127-2018 (Revision of IEEE Std C57.127-2007), doi: 10.1109/IEEESTD.2019.8664690.
12. Kozioł M., Boczar T., Nagi Ł. (2019), Identification of electrical discharge forms, generated in insulating oil, using the optical spectrophotometry method, *IET Science, Measurement & Technology*, **13**(3): 416–425, doi: 10.1049/iet-smt.2018.5059.
13. Kraetge A., Hoek S., Koch M., Koltunowicz W. (2013), Robust measurement, monitoring and analysis of partial discharges in transformers and other HV apparatus, *IEEE Transactions on Dielectrics and Electrical Insulation*, **20**(6): 2043–2051, doi: 10.1109/TDEI.2013.6678852.
14. Kundu P., Kishore N.K., Sinha A.K. (2012), Identification of two simultaneous partial discharge sources in an oil-pressboard insulation system using acoustic emission techniques, *Applied Acoustics*, **73**(4): 395–401, doi: 10.1016/j.apacoust.2011.11.004.
15. Kundu P., Kishore N.K., Sinha A.K. (2013), Frequency dependent propagation characteristics of partial discharge acoustic emission signal, *Proceedings of IEEE 1st International Conference on Condition Assessment Techniques in Electrical Systems, IEEE CATCON 2013*, Vol. I, pp. 227–230, doi: 10.1109/CATCON.2013.6737503.
16. Kunicki M., Cichon A. (2018), Application of a phase resolved partial discharge pattern analysis for acoustic emission method in high voltage insulation systems diagnostics, *Archives of Acoustics*, **43**(2): 235–243, doi: 10.24425/122371.
17. Kunicki M., Cichon A., Borucki S. (2018), Measurements on partial discharge in on-site operating power transformer: A case study, *IET Generation, Transmission and Distribution*, **12**(10): 2487–2495, doi: 10.1049/iet-gtd.2017.1551.
18. Kunicki M., Cichoń A., Borucki S. (2016), Study on descriptors of acoustic emission signals generated by partial discharges under laboratory conditions and in on-site electrical power transformer, *Archives of Acoustics*, **41**(2): 265–276, doi: 10.1515/aoa-2016-0026.
19. Kunicki M., Nagi L. (2017), Correlation analysis of partial discharge measurement results, *Proceedings of 17th IEEE International Conference on Environment and Electrical Engineering and 1st IEEE Industrial and Commercial Power Systems Europe*, (EEEIC / I and CPS Europe 2017), pp. 1–6, doi: 10.1109/EEEIC.2017.7977407.
20. Kunicki M. (2019), Variability of the acoustic emission signals generated by partial discharges in mineral oil, *Archives of Acoustics*, **44**(2): 339–348, doi: 10.24425/aoa.2019.128497.
21. Kunicki M., Cichoń A., Nagi Ł. (2018), Statistics based method for partial discharge identification in oil paper insulation systems, *Electric Power Systems Research*, **163**: 559–571, doi: 10.1016/j.epsr.2018.01.007.
22. Li Y. *et al.* (2013), Classification of partial discharge under different voltages using acoustic emission techniques, *Proceedings of IEEE International Conference on Solid Dielectrics, ICSD*, pp. 121–124, doi: 10.1109/ICSD.2013.6619854.
23. Mahmood Najafi S.A., Peimankar A., Saadati H., Gockenbach E., Borsi H. (2013), The influence of corona near to the bushing of a transformer on partial discharge measurement with an acoustic emission sensor, *Proceedings of 2013 IEEE Electrical Insulation Conference, EIC 2013*, pp. 295–298, doi: 10.1109/EIC.2013.6554253.
24. Mehdizadeh S., Yazdchi M., Niroomand M. (2013), A novel AE based algorithm for PD localization in power transformers, *Journal of Electrical Engineering and Technology*, **8**(6): 1487–1496, doi: 10.5370/JEET.2013.8.6.1487.
25. Mondal M., Kumbhar G.B. (2018), Detection, measurement, and classification of partial discharge in a power transformer: methods, trends, and future research, *IETE Technical Review (Institution of Electronics and Telecommunication Engineers, India)*, **35**(5): 483–493, doi: 10.1080/02564602.2017.1335244.
26. Murugan R., Ramasamy R. (2015), Failure analysis of power transformer for effective maintenance planning in electric utilities, *Engineering Failure Analysis*, **55**: 182–192, doi: 10.1016/j.engfailanal.2015.06.002.

27. Nicoară T., Marinescu A., Patru I. (2016), Partial discharge diagnostics in power and instrument transformer based on acoustic emission method, *Proceedings of 2016 International Conference on Applied and Theoretical Electricity, ICATE 2016*, pp. 1–6, doi: 10.1109/ICATE.2016.7754675.

28. Olszewska A., Witos F. (2012), Location of partial discharge sources and analysis of signals in chosen power oil transformers by means of acoustic emission method, *Acta Physica Polonica A*, **122**(5): 921–926, doi: 10.12693/APhysPolA.122.921.

29. Olszewska A., Witos F. (2011), Location and identification of acoustic signals recorded in power oil transformers within the band of 20–180 kHz, *Acta Physica Polonica A*, **120**(4): 709–712, doi: 10.12693/APhysPolA.120.709.

30. Olszewska A., Witos F. (2016), Identification of acoustic emission signals originating from the core magnetization of power oil transformer, *Archives of Acoustics*, **41**(4): 799–812, doi: 10.1515/aoa-2016-0077.

31. Rozga P. (2016), Using the light emission measurement in assessment of electrical discharge development in different liquid dielectrics under lightning impulse voltage, *Electric Power Systems Research*, **140**: 321–328, doi: 10.1016/j.epsr.2016.06.009.

32. Rubio-Serrano J., Rojas-Moreno M.V., Posada J., Martínez-Tarifa J., Robles G., García-Souto J. (2012), Electro-acoustic detection, identification and location of partial discharge sources in oil-paper insulation systems, *IEEE Transactions on Dielectrics and Electrical Insulation*, **19**(5): 1569–1578, doi: 10.1109/TDEI.2012.6311502.

33. Shang H., Lo K.L., Li F. (2017), Partial discharge feature extraction based on ensemble empirical mode decomposition and sample entropy, *Entropy*, **19**(9): 439, doi: 10.3390/e19090439.

34. Siegel M., Beltle M., Tenbohlen S., Coenen S. (2017), Application of UHF sensors for PD measurement at power transformers, *IEEE Transactions on Dielectrics and Electrical Insulation*, **24**(1): 331–339, doi: 10.1109/TDEI.2016.005913.

35. Sikorski W. (2019), Active dielectric window: A new concept of combined acoustic emission and electromagnetic partial discharge detector for power transformers, *Energies*, **12**(1): 115, doi: 10.3390/en12010115.

36. Tenbohlen S., Coenen S., Djamali M., Müller A., Samimi M.H., Siegel M. (2016), Diagnostic measurements for power transformers, *Energies*, **9**(5): 1–25, doi: 10.3390/en9050347.

37. Veloso G.F.C., Da Silva L.E.B., Noronha I., Lambert-Torres G. (2008), Identification of wavefronts in Partial Discharge acoustic signals using discrete Wavelet Transform, *Proceedings of IEEE International Symposium on Industrial Electronics*, pp. 1003–1008, doi: 10.1109/ISIE.2008.4677219.

38. Witos F., Gacek Z. (2005), Application of the calibrated acoustic emission to investigate properties of acoustic emission signals coming from partial discharge sources modelled in laminar systems, *Journal de Physique IV (Proceedings)*, **129**: 173–177, doi: 10.1051/jp4:2005129037.

39. Witos F., Olszewska A., Szerszeń G. (2011), Analysis of properties characteristic for acoustic emission signals recorded on-line in power oil transformers, *Acta Physica Polonica A*, **120**(4): 759–762, doi: 10.12693/APhysPolA.120.759.

40. Yaacob M.M., Alsaedi M.A., Rashed J.R., Dakhil A.M., Atyah S.F. (2014), Review on partial discharge detection techniques related to high voltage power equipment using different sensors, *Photonic Sensors*, **4**(4): 325–337, doi: 10.1007/s13320-014-0146-7.